

Simple Synthesis of Carboxylate–Rich Porous Carbon Microspheres for High-Performance Supercapacitor Electrode Materials

Chenglong He¹, Yingliang Liu^{2,*}, Zhiping Xue¹, Mingtao Zheng^{2,*}, Haibo Wang¹, Yong Xiao², Hanwu Dong², Haoran Zhang², Bingfu Lei²

¹Department of Chemistry, Jinan University, Huanpu Avenue Western 601[#], Tianhe District, Guangzhou 510632, China

² Department of Applied Chemistry, College of Science, South China Agricultural University, Wushan Road 483[#], Tianhe District, Guangzhou 510642, China

*E-mail: tliuyl@163.com; mtzheng@scau.edu.cn

Received: 19 March 2013 / Accepted: 13 April 2013 / Published: 1 May 2013

Carboxylate–rich porous carbon microspheres with high specific surface area were synthesized via a simple hydrothermal carbonization method by using starch and acrylic acid as starting materials, followed by steam activation at 800 °C in nitrogen atmosphere for 1 h. The resulting materials were characterized using various methods including, X–ray diffraction (XRD), Raman spectrum, infrared spectrum (FTIR), X-ray photoelectron spectroscopy (XPS), scanning electron microscope (SEM), and BET measurements. Cyclic voltammetry and galvanostatic charge/discharge experiments were adopted to investigate their electrochemical behaviors. The cyclic voltammetry (CV) measurement shows that the synthesized porous microspheres exhibited a super capacitance of 190 F g⁻¹ at the scanning rate of 2 mV s⁻¹. The galvanostatic charge/discharge shows it exhibited a large specific capacitance up to 212 F g⁻¹ with the current density of 0.5 A g⁻¹. The experimental results indicate that carboxyl groups and high surface area could enhance both specific capacitance and electrochemical stability of the resultant microspheres.

Keywords: Carboxylate–rich porous carbon, high specific surface area, super capacitance

1. INTRODUCTION

Supercapacitors, also called as electrical double layer capacitors (EDLCs), have steadily grown in importance as high–power electrochemical energy storage devices owing to their advantages such as ultra-long cycle-life, sub-second charging, and a very wide operational temperature range, properties that are currently unattainable in Li–ion batteries [1–6]. These devices are of great promise in various

fields in consumer electronics, uninterruptable power supplies, energy efficient industrial equipment, electric and hybrid electric vehicles and power grid applications [1, 2].

Energy storage in supercapacitors is based on the electrostatic adsorption of electrolyte ions on the large specific surface area of electrically conductive porous electrodes. In spite of the higher capacitance often offered by conductive polymers [7] and metal oxide-based supercapacitors [8, 9], the greater cycle stability and higher electrical conductivity of porous carbons has resulted in their use in nearly 100% of commercial devices. It has been demonstrated that multiple factors affected the performance of carbon-based supercapacitors. To date, the most important factor is the carbon electrodes' surface chemistry, specific surface area, and their pore size distribution [10–17]. The ideal pores should be slightly larger than the size of the de-solvated ions. Smaller pores prevent efficient ion electro-adsorption [15], whereas significantly larger pores reduce the capacitance [16]. Only the co-existence of large mesopores with micropores in carbons is required for rapid ion transport and high power characteristics of supercapacitors [17].

Various porous carbon microspheres have been successfully synthesized via template techniques [18–20], catalytic activation [21–23], carbonization of polymer blend [24], and CVD methods [25], etc. However, these methods have a complicated synthesis procedure or are of high cost or using certain toxic reagents. Furthermore, the surface area, the surface groups, and the mesopore rate of the porous carbons are relatively low, resulting in the low capacitance. Herein, we develop a two-step method including the hydrothermal carbonization of starch in the presence of acrylic acid and then activated by steam, to prepare a kind of porous carbon microspheres with enhanced electrochemical performance. In our study, the starch is used as carbon source, the acrylic acid provide carboxyl group and also help to create more mesopores on the surface of carbon microspheres, then the steam activation enlarge the surface area of the carbon microspheres. Experimental results show that the carbon microspheres exhibited a super capacitance up to 190 F g^{-1} at the scanning rate of 2 mV s^{-1} in the cyclic voltammeter (CV) measurements and exhibited a good electro cycling stability.

2. EXPERIMENTAL SECTION

2.1 Synthesis of carboxylate-rich porous carbon microspheres.

All the chemical reagents were analytically pure and used without further purification. To obtain porous carbon microspheres with a different degree of carboxylic groups, acrylic acid has been added as a co-monomer to the reaction mixture. Different ratios (0, 15, 30, and 45 wt %) with respect to the total starch concentration have been employed. starch is used as carbon source and its concentration in deionized water is 10 w/v %. The solution was then transferred into a 50 ml Teflon-lined stainless-steel autoclave and hydrothermally treated at $180 \text{ }^\circ\text{C}$ for 20 h. The resulting powder was collected by centrifugation, and washed with deionized water. Subsequently the powder was activated by steam at $800 \text{ }^\circ\text{C}$ for 60 min. The resulting carboxylate-rich porous carbon microsphere samples were labeled according to the acrylic acid monomer concentration added into the reaction mixture. For

instance, Pure-S, A-S15%, A-S30%, and A-S45% correspond to 0, 15, 30, and 45 wt %, respectively, of acrylic acid used in the reaction media.

2.2 Characterization of carboxylate-rich porous carbon microspheres.

The structure of the as-prepared samples was analyzed by a MSAL-XD2 X-ray diffractometer (XRD, Cu K α , 36 kV, 20 mA, $\lambda = 0.154\ 06\ \text{nm}$). The Raman spectrum of the as-prepared samples was recorded at room temperature on a Renishaw RM2000 Raman microspectrometer with the 514.5 nm line of an argon laser. Fourier transform infrared ray (FTIR) spectra were recorded using a Varian 600 Spectrometer. X-ray photoelectron spectroscopy (XPS) was carried out by means of a Specs spectrometer, using Mg K α (1253.6 eV) radiation emitted from a double anode at 50 W. Binding energies for the high-resolution spectra were calibrated by setting C 1s at 284.6 eV. The morphologies were observed on a Philips SEM-XL30S scanning electron microscope. The specific surface area was measured via the Micromeritics TriStar 3000 analyzer.

2.3 Electrochemical tests.

The working electrode was prepared by pressing the mixture of carboxylate-rich porous carbon microspheres, carbon black and 5% PTFE (75:15:10wt %) into a foam nickel electrode under 35 MPa. All electrochemical measurements were conducted in a standard three electrodes cell on a CHI 660B electrochemical workstation in an aqueous solution of 6 mol L $^{-1}$ KOH. Different sweep rates were employed in cyclic voltammeter within the range from -0.9V to 0.1 V vs Hg/HgO.

3. RESULTS AND DISCUSSION

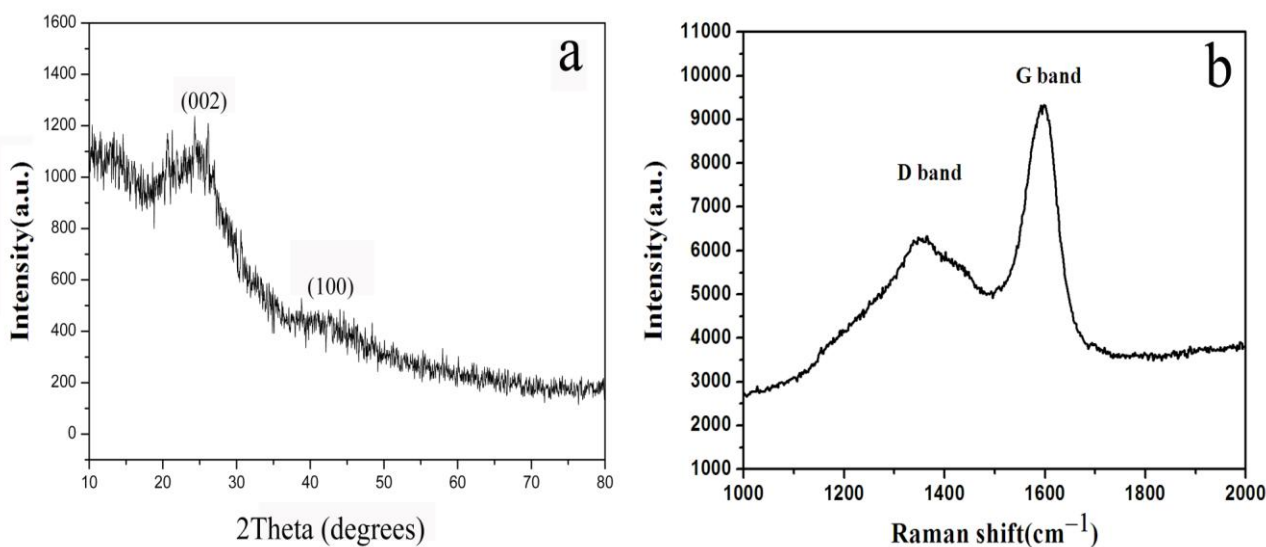


Figure 1. XRD pattern (a) and Raman spectrum (b) of the obtained carbon microspheres.

3.1. XRD pattern and Raman spectrum of the obtained carbon microspheres.

Fig. 1a shows the XRD patterns of the as-prepared sample, there is broad peak at 24° which corresponds to the (002) plane of graphite. In addition, a small shoulder peak at 44° which corresponds to the (100) plane of graphite, can be observed. The broadening of the two peaks suggests the possible presence of an amorphous carbon phase [26] within the carbonaceous materials.

Fig. 1b shows the micro-Raman spectrum of the as-prepared sample. Two strong peaks at 1332 and 1595 cm^{-1} can be seen. The peak at 1592 cm^{-1} (G band) is attributed to an E_{2g} mode of graphite and is related to the vibration of sp^2 -bonded carbon atoms in a 2D hexagonal lattice, such as in a graphite layer. The peak at 1333 cm^{-1} (D band) corresponds to vibrations of carbon atoms with dangling bonds in plane terminations of disordered graphite. The D and G bands show an intensity ratio of $I_D/I_G = 0.89$ for the carbonaceous materials [27]. This intensity ratio indicates an amorphous carbon structure, with a high content of lattice edges or plane defects within the analyzed carbonaceous materials, which is consistent with the XRD results. Moreover, the D band has a much wider width in the present observation. The spectrum is more characteristic of disordered graphite owing to the lower carbonization temperature.

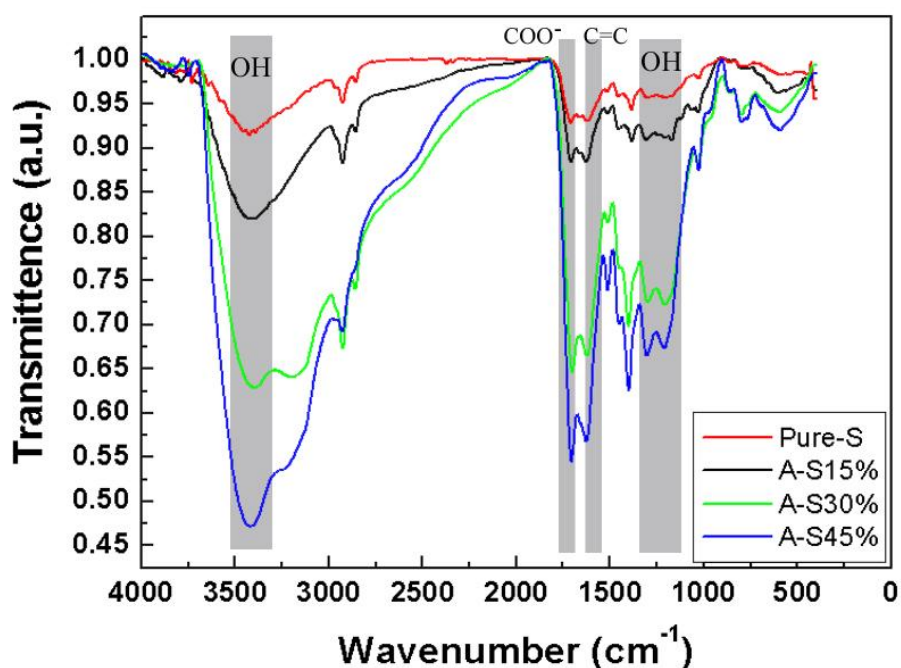


Figure 2. FTIR spectra pure-S and the resultant carboxylate-rich samples.

3.2. FT-IR analysis of the obtained carbon microspheres.

The presence of carboxylic groups on the surface of the samples was proved by using FTIR spectroscopy. The FTIR spectra of the Pure-S and all the resulting materials are shown in Fig. 2. Upon hydrothermal carbonization of starch, carbon materials rich in functional groups such as hydroxyl,

esters, carbonyl, and carboxylic groups are obtained. It can be observed that the intensity of the adsorption band at around 1700 cm^{-1} , corresponding to the carboxylate group, increases upon increasing the amount of acrylic acid in the sample, proving a higher degree of carboxylic groups in the modified materials, similar to that of carboxylate-rich carbon microspheres from hydrothermal carbonization of glucose [28]. The other adsorption bands belong to C=C double bonds (1620 cm^{-1}), C–OH stretching and OH bending vibrations ($1000\text{--}1300\text{ cm}^{-1}$), the latter underlining also confirms the existence of a large number of residual hydroxyl groups constituting the hydrophilic surface.

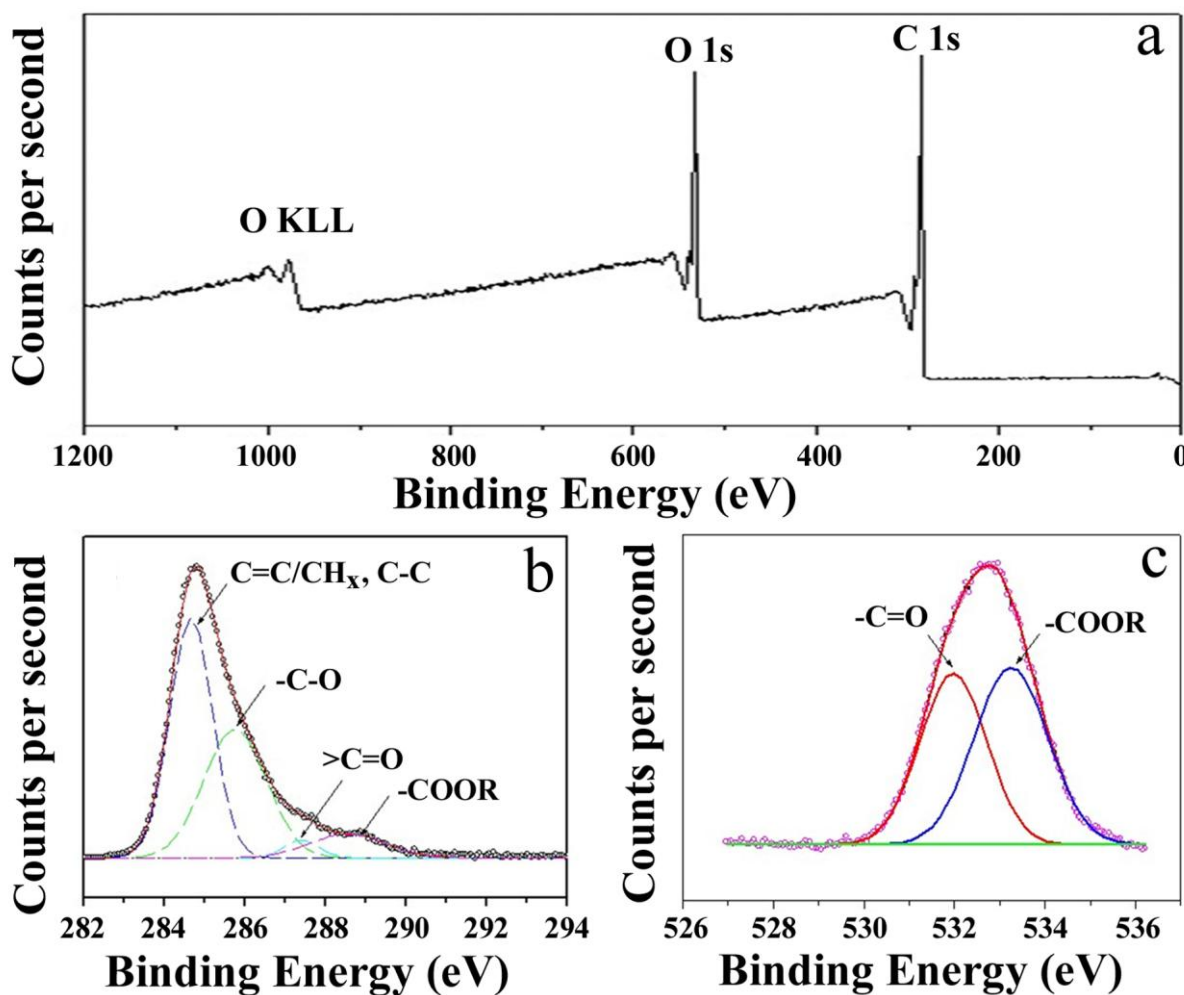


Figure 3. XPS spectra of carboxylate-rich samples (a), Peak split of C 1s (b) and O 1s (c).

3.3 XPS analysis of carboxylate-rich samples.

X-ray photoelectron spectroscopy (XPS) was used to characterize the oxygen functionalities present on the outer layer (shell) of the carbon microspheres. As a representative example, Fig. 3a shows the C 1s and O 1s core-level spectra of the carboxylate-rich samples, and the peak-fitting of the C 1s and O 1s envelopes. For the C 1s spectrum represented in Fig. 3b, four signals at 284.5, 285.8, 287.4, and 289.1 eV were identified, which can be attributed to carbon group (C=C, CH_x, C-C), hydroxyl groups or ethers (-C-OR), carbonyl or quinone groups (>C=O), and carboxylic groups, esters,

or lactones(-COOR), respectively. The presence of these oxygenated groups was confirmed by the O 1s spectrum (Fig. 3c), in which two signals were identified at 531.8 and 533.2 eV. The former corresponds to C=O groups, while the peak at 533.0 eV is mainly attributed to -C-O- groups, although a certain contribution from -COOR is probably also present, as evidenced by the C 1s envelope [29].

3.4 SEM analysis of carboxylate-rich samples.

Fig. 4 shows the morphologies of the carbon microspheres. From the Fig. 4a, it is shown that upon hydrothermal carbonization of pure starch, micrometer sized, microporous carbon spheres with smooth surfaces are obtained. From Fig. 4b-f, we can see that addition of acrylic acid induces a change in the particle morphology, that is, the surface of the particles is no longer smooth and the microspheres indicate that they are formed out of small aggregated particles, just like “the Halley Comet”. This effect is more pronounced when more acrylic acid is added into the system. Upon addition of only 15 wt % acrylic acid, some of the spheres possess this morphology, whereas the others appear smooth like in the case of Pure-S. In this case, the amount of acrylic acid was probably not sufficient in order to be incorporated in all intermediary particles formed during the hydrothermal carbonization. Lately formed particles may be depleted in acrylic acid and progress via the classical hydrothermal carbonization route.

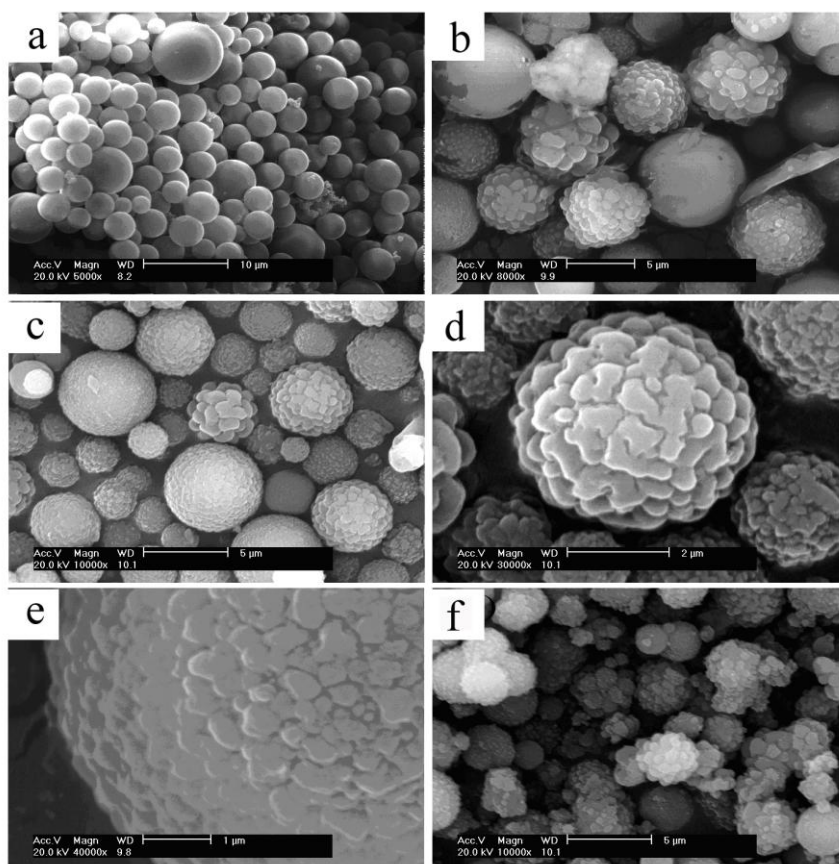


Figure 4. SEM micrographs of Pure-S (a), A-S15% (b), A-S30% (c-e) and A-S45% (f).

3.5. Specific surface area analysis of carboxylate-rich samples.

The A-S30% material shows monodisperse micrometer-sized spheres formed out of a uniform aggregate of nanosized spheres. It seems that the amount of acrylic acid is in this case optimal for producing such uniform superstructures. Once the acrylic acid amount is increased up to 45%, the morphologies of the carbon microspheres turn broken. Fig. 5 shows the nitrogen adsorption-desorption isotherms of A-S30% and pure-S, and the specific surface area and pore structure parameters of the as-synthesized samples as shown in Table 1. The A-S30% exhibit a type IV sorption isotherm with a sharp capillary condensation step and a hysteresis loop near relative pressure of ~0.5 in the desorption branch indicates the presence of mesopores [30]. The pure-S exhibit a type I sorption isotherm, which means most pores in the pure-S are micropores. The BET surface area of A-S30% is 1036 m² g⁻¹, which is much higher than those of the pure-S (597 m² g⁻¹). The A-S30% pore size distribution curve (Fig. 5 inset) shows its pores with detectable sizes of about 3.5 nm, which belongs to mesopores.

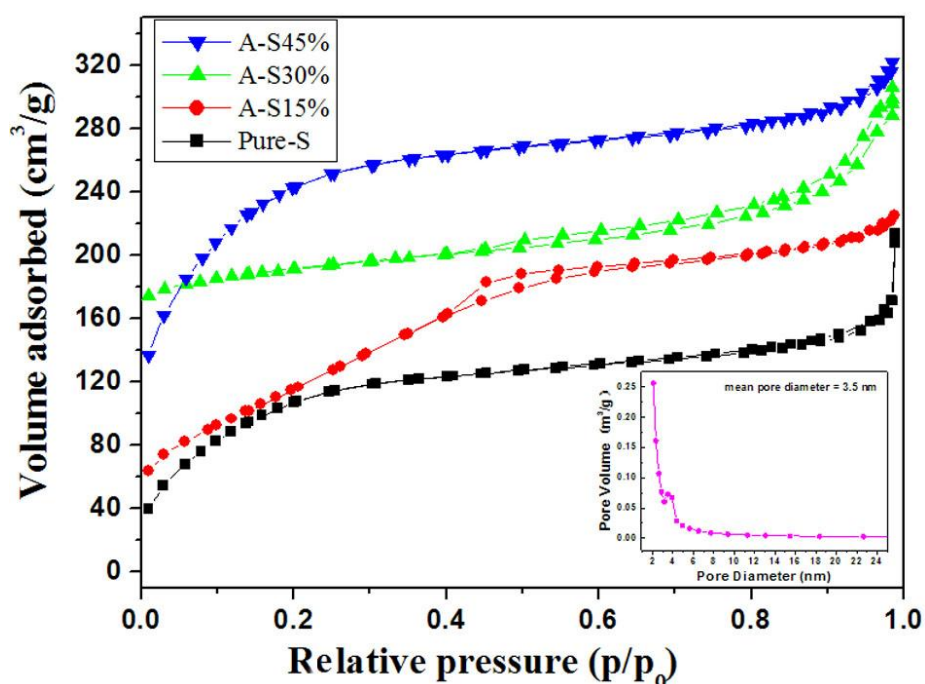


Figure 5. Nitrogen sorption isotherms of A-S30% and pure-S. The inset is A-S30% pore size distribution curve.

Table 1. Specific surface area and pore structure parameters of the as-synthesized samples.

Samples	S _{BET} m ² g ⁻¹	V _{TPV} cm ³ g ⁻¹	D _{BJH} nm
A-S45%	1148	0.58	1.41
A-S30%	1036	0.64	3.54
A-S15%	785	0.43	2.48
Pure-S	597	0.33	1.76

3.6. Electrochemical behavior of carbon microspheres electrode.

To investigate the electrochemical performance of the resultant carbon microspheres, we have employed two electrochemical methods involving cyclic voltammetry and galvanostatic charge/discharge. The cyclic voltammograms (CV) of the sample pure-S, A-S15%, A-S30% and A-S45% in 6 mol L⁻¹ KOH at 20 mV s⁻¹ scan rate are shown in Fig. 6a. It is well known that an ideal capacitance behavior of a carbon material electrode is expressed in the form of a rectangular shape on the voltammetry characteristics [31]. From the Fig. 6a, the CV of pure-S shows a sharply distorted but with the more acrylic acid is added into the system, the more regular rectangular shape we will get. The rectangular-like shape and the appearance of humps (around -0.7 V) in the CV curves of A-S30% indicate that the capacitive response comes from the combination of EDLC and redox reactions, which is related to the pseudocapacitive effect of the oxygen-containing functional group such as carboxylic group [32]. Note that the slopes of current variation near the vertex potentials are almost vertical at CV, illustrating the excellent behaviour of A-S30% as electrode materials with very small equivalent series resistance. However, when the ratio of acrylic acid reached 45%, the sharp of CV turn worse.

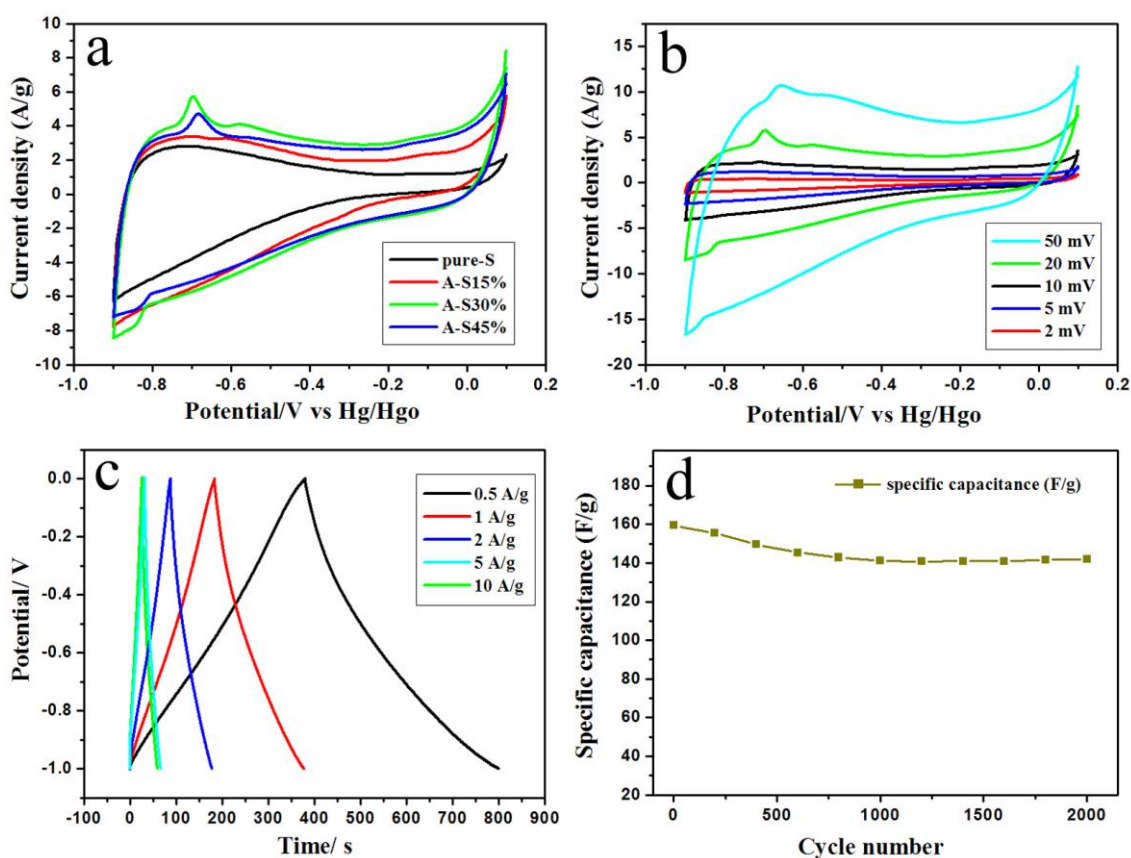


Figure 6. (a) Cyclic voltammograms (CV) of the sample pure-S, A-S15%, A-S30% and A-S45% in 6 mol L⁻¹ KOH at 2 mV s⁻¹ scan rate. (b) CVs of A-S30% in 6 mol L⁻¹ KOH at different scan rate. (c) Galvanostatic charge/discharge curves of A-S30% in 6 mol L⁻¹ KOH at different current density. (d) Cycle life for A-S30% measured at 20 mV s⁻¹.

Table 2. Specific capacitance (C) measurements of different samples at 20 mV s⁻¹.

sample	pure-S	A-S15%	A-S30%	A-S45%
C(F g ⁻¹)	82	121	160	143

The specific capacitances (C) of electrodes are calculated according to the following equation from the measured CVs:

$$C = \frac{Q}{wv} = \frac{\int idt}{w\Delta v} \quad (1)$$

Where i , w and Δv are the sample current, the weight of active materials and the voltage window, respectively. The data calculated from CVs of carbon microspheres is summarized in Table 2. The sample pure-S made by pure starch shows low specific capacitance of 82 F g⁻¹, but when acrylic acid was added into the system, the specific capacitance of carbon microspheres have been greatly improved. A maximum capacitance of 160 F g⁻¹ at 20 mV s⁻¹ can be obtained when the ratio of acrylic acid reached 30%. Probably, the higher capacitance of A-S30% may be due to that the additive of acrylic acid may create more pores, which helps increasing the surface area of carbon microspheres. On the other hand, the sample of A-S30% exhibits a more active surface since a large number of surface functional groups such as carboxylic group are presented on their surface, which is similar to the functionalized carbon nanotubes [33]. It was found that the surface area of A-S30% is 1036 m² g⁻¹, while the pure-S is only 597 m² g⁻¹. However, when the ratio of acrylic acid reached 45%, as can be seen in A-S45%, the specific capacitance decreases. This is because the specific capacitance increasing is not only by the specific surface area of materials for electrolyte accessibility but also by the number of mesopores. The ratio of 30% acrylic acid create more mesopores, when the ratio continues to increase, acrylic acid may create micropores instead.

Table 3. Specific capacitance(C) measurements of A-S30% at different scan rate.

sweep rate (mV s ⁻¹)	50	20	10	5	2
C (F g ⁻¹)	133	160	168	176	190

As can be seen from Fig. 6b and Table 3, with the reduce of sweep rate, the sharp of CVs turn to be a better rectangle and the specific capacitance measurement increase, up to about 190 F g⁻¹ at the scan rate of 2 mV s⁻¹.

The galvanostatic charge/discharge measurements are performed with various current densities in order to further investigate the performances of as synthesized products (Fig. 6c). The specific capacitance (C) of the samples was calculated according to the following equation:

$$C = \frac{it}{w\Delta v} \quad (2)$$

where i , t , w and Δv are the constant current and discharge time and the weight of active materials and the voltage window, respectively.

Table 4. Galvanostatic charge/discharge measurements of A-S30% at various current densities.

Current density(A g ⁻¹)	5	2	1	0.5
Capacitance(F g ⁻¹)	170	181	195	212

The charge/discharge curves of A-S30% are linear and symmetrical, and the IR drop is not obvious, which shows good capacitance, highly reversible charge/discharge efficiency. The capacitance of A-S30% can up to 212 F g⁻¹ at 0.5 A g⁻¹ current density (Table 4).

The cyclic voltammetry experiments were performed at a sweep rate of 20 mV s⁻¹ for 2000 cycles in order to investigate the cycling stability of A-S30% (Fig. 6d). The specific capacitance of A-S30% is to a 160 F g⁻¹ for the first cycle and the 147 F g⁻¹ after 2000 cycles. Over 90% of the original specific capacitance remained for A-S30%, indicating the good electrochemical stability of the as-synthesized carbon microspheres.

4. CONCLUSIONS

In summary, carboxylate-rich porous carbon microspheres were synthesized successfully via simple hydrothermal carbonization of starch in the presence of acrylic acid, and then followed with a steam activation process at 800 °C in nitrogen atmosphere. The resultant carbon microspheres were in rich of carboxylate groups in the surface and presented high surface area and pore size of 3.5 nm. The CV measurement shows that the synthesized microspheres exhibited a super capacitance of 190 F g⁻¹ at the scan rate of 2 mv s⁻¹. The galvanostatic charge/discharge shows it exhibited a large specific capacitance up to 212 F g⁻¹ with the current density of 0.5 A g⁻¹. The experimental results indicate that carboxyl groups and high surface area could enhance both specific capacitance and electrochemical stability of the resultant microspheres.

ACKNOWLEDGEMENTS

The financial support for this work provided by the National Science Foundation of China (21031001, 21201065), the Natural Science Foundation (s2012040007836), the Key Program of Science Technology Innovation Foundation of Universities (cxzd1014) of Guangdong Province and the Science and Technology Plan Projects of Guangdong Province (2011A081301018) is gratefully acknowledged.

References

1. P. Simon, Y. Gogotsi, *Nature Mater.*, 7(2008) 84.
2. J.R. Miller, P. Simon, *Science*, 321(2008) 651.
3. M. Jayalakshmi, K. Balasubramanian, *Int. J. Electrochem. Sci.*, 3(2008)1196
4. J.R. Miller, R.A. Outlaw, B.C. Holloway, *Science*, 329(2010)1637
5. A. Kajdos, A. Kvit, F. Jones, J. Jagiello, G. Yushin, *J. Am. Chem. Soc.*, 132(2010) 3252
6. D. Pech, M. Brunet, H. Durou, P. H. Huang, V. Mochalin, Y. Gogotsi, P. L. Taberna, P. Simon *Nature nanotechnol.*, 5(2010) 651
7. I. Kovalenko, D. Bucknall, G. Yushin, *Adv. Funct. Mater.*, 20(2010)3979
8. G.R. Fu, Z.A. Hu, L.J. Xie, *Int. J. Electrochem. Sci.*, 4(2009)1052
9. F. Zhang, L. Hao, L. J. Zhang, X. G. Zhang, *Int. J. Electrochem. Sci.*, 6(2011)2943
10. C. Portet, G. Yushin, Y. Gogotsi, *Carbon*, 45(2007)2511
11. C. O. Ania, V. Khomenko, E. Raymundo-Pinero, J. B. Parra, F. Beguin, *Adv. Funct. Mater.*, 17(2007) 1828
12. D. Hulicova-Jurcakova, M. Seredych, G.Q. Lu, T. J. Bandosz, *Adv. Funct. Mater.*, 19(2009) 438
13. J. Chmiola, G. Yushin, Y. Gogotsi, C. Portet, P. Simon, *Science* 313(2006) 1760
14. B. B. Garcia, S.L. Candelaria, G. Cao, *Journal of Materials Science* 47(2012)5596
15. L. Eliad, E. Pollak, N. Levy, G. Salitra, A. Soffer, D. Aurbach, *Appl. Phys. A*, 82(2006)607
16. G. Salitra, A. Soffer, L. Eliad, Y. Cohen, D. Aurbach, *J. Electrochem. Soc.*, 147(2000) 2486
17. E. Raymundo-Pinero, K. Kierzek, J. Machnikowski, F. Beguin, *Carbon*, 44(2006)2498
18. J. Lee, S. Yoon, S. M. Oh, C.H. Shin, T. Hyeon, *Adv. Mater.*, 12(2000)359
19. J. S. Lee, S. H. Joo, R. Ryoo, *J. Amer. Chem. Soc.*, 124(2002) 1156
20. J. Górka, A. Zawislak, J. Choma, M. Jaroniec *Carbon*, 46(2008)1159
21. M. Gozin, A. Weisman, Y. Ben-David, D. Milstein, *Nature*, 364(1993)699
22. J.F. Sun, X.Q. Wang, C. Wang, Q. Wang, *J. Appl. Polymer*, 99(2006) 2565
23. H. Tamon, H. Ishizaka, M. Okazaki, *Carbon*, 35(1997)791
24. H.Y. Liu, K.P. Wang, H.S. Teng, *Carbon*, 43(2005)559
25. K. Kobayashi, R. Kitaura, Y. Kumai, Y. Goto, S. Imagaki, H. Shinohara, *Carbon*, 47(2009)722
26. H.B. Chen, H.B. Wang, M.T. Zheng, Y.L. Liu, *Int. J. Electrochem. Sci.*, 7(2012)4889
27. M.T. Zheng, Y.L. Liu, Y. Xiao, *J. Phys. Chem. C.*, 113(2009) 8455
28. R. Demir-Cakan, N. Baccile, M. Antonietti, M.M. Titirici, *Chem. Mater.*, 21(2009)484
29. K. Zhong, Z.T. Lin, X.L. Zheng, G.B. Jiang, *Carbohydr. Polym.*, 92(2013)1367
30. E.G. Calvo, J.A. Menéndez, A. Arenillas, *Microporous Mesoporous Mater.*, 168(2013)206
31. N.N. Xia, T.X. Zhou, S.S. Mo, *J. Appl. Electrochem.*, 41(2011)71
32. E. Raymundo-Piñero, F. Leroux, F. Béguin, *Adv. Mater.*, 18 (2006)1877
33. J. Yang, S. C. Wang, X. Y. Zhou, J. Xie, *Int. J. Electrochem. Sci.*, 7(2012)6118